

Short communication

Nano Scale Magnetically Recoverable Supported Heteropoly Acid as an Efficient Catalyst for the Synthesis of Benzimidazole Derivatives in Water

Ezzat Rafiee,* Nasibeh Rahpeima and Sara Eavani

Faculty of Chemistry, Razi University, Kermanshah, 67149, Iran

* Corresponding author: E-mail: ezzat_rafiee@yahoo.com; Tel/Fax: 098-831-4274559

Received: 09-03-2013

Abstract

12-Tungstophosphoric acid supported on silica-coated magnetic nano particles was prepared and characterized by transmission electron microscopy, scanning electron microscopy, powder X-ray diffraction and inductively coupled plasma atomic emission spectroscopy. Acidity of the catalysts was measured by potentiometric titration with n-butylamine. Catalytic activity of the prepared sample was evaluated in the model synthesis of 1,2-disubstituted benzimidazole derivatives in water. The catalyst showed excellent catalytic activity and the corresponding products were obtained in good to excellent yields under mild reaction conditions. Furthermore, the catalyst could be easily recovered using an external magnet and reused several times. The leaching and surface acidity of the recovered catalyst were also investigated.

Keywords: Magnetic materials, nano structures, benzimidazole, heterogeneous catalyst, heteropoly acid.

1. Introduction

Catalysis plays an important role in clean technology. The application of new catalysts and catalytic systems can simultaneously achieve the dual goals of environment protection and economic benefits. New synthetic methods are constantly developed with the idea of improving or replacing older non- or less-green technologies. The application of Keggin type heteropoly acids (HPAs) as catalysts has now been extended to the synthesis of fine chemicals like drugs and drug intermediates to response the objections of environmental pollution and corrosion of the traditional technologies.^{1–5} Supported HPAs are important for many applications because bulk HPAs have low specific surface area (1–10 m²/g). Supports with high specific surface area, such as nano particles (NPs), or mesoporous materials, are of special interest, because the number of accessible acid sites has been increased.^{6,7} However, decreasing the diameter of the supported particles down to the nanometer scale increase the problems of catalyst separation and recycling that are essential steps in nano-catalytic technology, and frequently affect the overall economy of the process. This problem can be solved

by using magnetic NPs as a support, which can be separated from the reaction mixture by using a magnetic field.^{8–11} Among various magnetic NPs, silica coated γ -Fe₂O₃ NPs, has been considered as an ideal candidate owing to its high surface area, surface modification ability, easy synthesis, and low toxicity.¹²

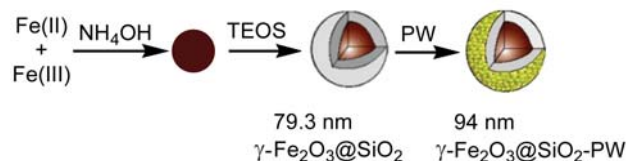
Benzimidazole derivatives play an important role in the drug discovery process due to their potential applications in the pharmaceutical industry.^{13–16} In spite of the availability of many methods for the synthesis of these compounds,^{17–27} there are still many drawbacks such as the use of highly toxic reagent, strong acids and, in some cases, harsh reaction conditions. Furthermore, most of these procedures generate mono-substituted benzimidazoles as a target product. Therefore, the search for new readily available green catalysts is still being actively pursued.

In the present work, we have demonstrated the use of a special magnetically recoverable heterogeneous HPA catalyst for the synthesis of biologically useful building blocks, 1,2-disubstituted benzimidazole derivatives, in water. We hope that this special catalyst may be a new promising candidate in the synthesis of other biologically active compounds in aqueous media.

2. Results and Discussion

2. 1. Characterization of the Catalyst

In order to obtain the silica coated $\gamma\text{-Fe}_2\text{O}_3$ NPs with small and narrow size distributions, various techniques for their preparation have been reported. A simple ferric oxide, $\gamma\text{-Fe}_2\text{O}_3$, was used as the magnetic material because of its low price, simplicity and non-toxicity. It was prepared through chemical co-precipitation method. The obtained $\gamma\text{-Fe}_2\text{O}_3$ NPs was subsequently coated with silica shell using the Stöber process.²⁸ In this process, the silica shell is formed during the hydrolysis of tetraethylorthosilicate (TEOS) in an ethanol solution containing water and ammonia. After the surface coating by SiO_2 , magnetic solid (designed as $\gamma\text{-Fe}_2\text{O}_3@ \text{SiO}_2$) was used as support for immobilization of 12-tungstophosphoric acid, $\text{H}_3\text{PW}_{12}\text{O}_{40}$



Scheme 1. Preparation of the nano catalyst.

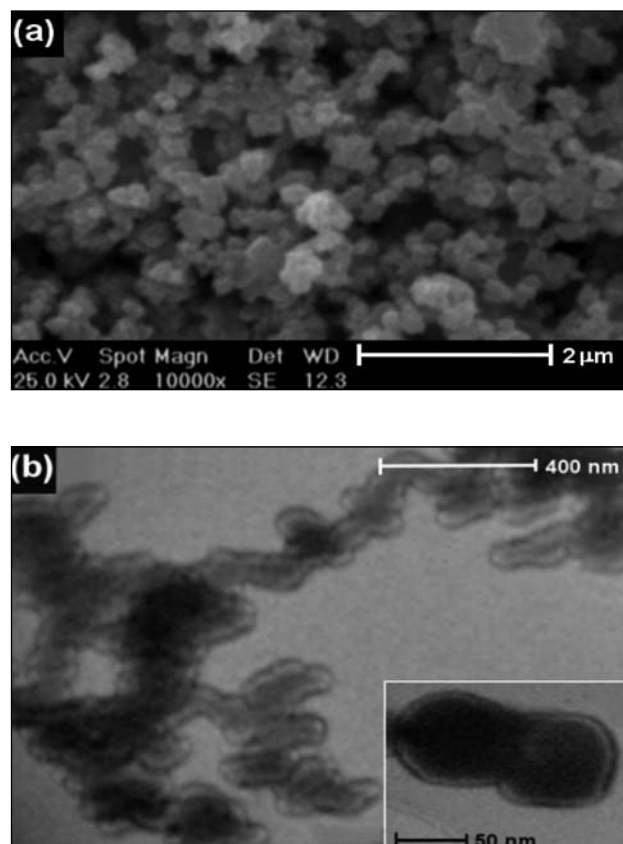


Figure 1. (a) SEM and (b) TEM images of $\gamma\text{-Fe}_2\text{O}_3@ \text{SiO}_2\text{-PW}$ catalyst.

(PW). The obtained catalyst, designed as $\gamma\text{-Fe}_2\text{O}_3@ \text{SiO}_2\text{-PW}$, was collected by attaching an external magnet and dried (Scheme 1).

Surface area of the catalyst was measured using the Braunauer, Emmet and Teller (BET) method. The results of BET method showed that the average surface area was $103 \text{ m}^2\text{g}^{-1}$ for $\gamma\text{-Fe}_2\text{O}_3@ \text{SiO}_2\text{-PW}$ catalyst. The morphological and structural features of the catalyst sample were investigated using transmission electron microscopy (TEM) and scanning electron microscopy (SEM) techniques (Figure 1). The catalyst had a uniform and spherical morphology with well-defined core-shell structure. The average particle size of $\gamma\text{-Fe}_2\text{O}_3@ \text{SiO}_2\text{-PW}$ catalyst was about 95 nm. The X-ray diffraction (XRD) pattern for the catalyst is shown in Figure 2. Silica exhibits broad band centered at $2\theta = 25^\circ$ and $\gamma\text{-Fe}_2\text{O}_3$ displays typical sharp peaks at $2\theta = 30.4^\circ$, 35.5° , 55.7° , and 62.5° . PW displays reflections at $2\theta = 9.7^\circ$ and 26.3° .^{29,30} The presence of the intense peaks indicates that there is no significant change in the structure of the PW and its crystalline character retained after immobilization on the support.

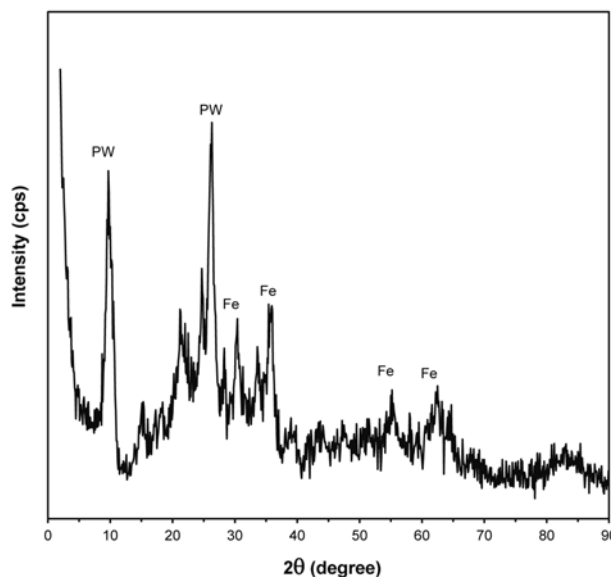
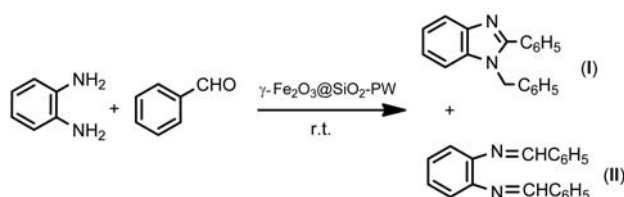


Figure 2. XRD patterns of $\gamma\text{-Fe}_2\text{O}_3@ \text{SiO}_2\text{-PW}$ catalyst.

2. 2. Catalytic Reaction

1,2-Phenylenediamine and benzaldehyde were selected as model substrates for optimization of the reaction conditions (Scheme 2). Different solvents including CH_3CN , $\text{C}_2\text{H}_5\text{OH}$, CHCl_3 , H_2O , and H_2O /sodium dodecyl sulfate (SDS) were used in the model reaction. The best result was obtained using $\text{H}_2\text{O}/\text{SDS}$ as solvent (Table 1). To evaluate the effect of SDS concentration, the reaction was carried out in the presence of different amounts of SDS. By using high amounts of the SDS, 1,2-disubstitu-

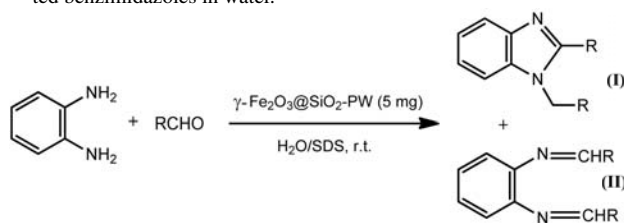
ted benzimidazole (I) was obtained as the main product in long reaction time. The catalyst amount was also optimized. It should be noted that when using a higher (0.15 mol %) or lower (0.03 mol %) amount than 0.07 mol % of the catalyst, the product (I) was obtained with low selectivity. We concluded that 0.07 mol % of the catalyst was the optimum amount for that reaction. When PW was used as the catalyst under optimized conditions, the desired product (I) was obtained in good yield. However, the imine (II) was also produced (Table 1, entry 10).



Scheme 2. Model reaction.

Using the above optimized reaction conditions, the reaction of various aldehydes and 1,2-phenylenediamine were investigated (Table 2). A series of aldehydes reacted with 1,2-phenylenediamine at room temperature to afford a wide range of benzimidazole derivatives in good to excellent yields. The results revealed that the electronic nature of the substituent on the phenyl ring had a significant effect on the yield and reaction time. Benzaldehydes with electron donating groups produced the corresponding benzimidazoles in good to excellent yields (entries 3–5). The study indicated that 3-hydroxy-benzaldehyde reacted very well and faster than 2-hydroxy-benzaldehyde (entries 6 and 7). Benzaldehydes bearing electron withdrawing groups (entries 10 and 11) gave only trace amounts of target product (product I). Furthermore, cyclohexylcarbaldehyde (entry 12) gave the corresponding benzimidazole in good yield, but in a longer reaction time, while aliphatic aldehydes and cinnamaldehyde were unreactive (entries 15 and 16).

Table 2. $\gamma\text{-Fe}_2\text{O}_3@\text{SiO}_2\text{-PW}$ catalyzed synthesis of 1,2-disubstituted benzimidazoles in water.



Entry	R	Time (min)	Yield (%) ^a		Ref.
			Product I	Product II	
1	C ₆ H ₅	5	95	–	16
2	4-Cl-C ₆ H ₄	25	94	–	25
3	4-isopropyl-C ₆ H ₄	45	95	–	26
4	4-CH ₃ -C ₆ H ₄	90	81	–	16
5	4-N(CH ₃) ₂ -C ₆ H ₄	75	70	–	16
6	3-OH-C ₆ H ₄	75	91	–	26
7	2-OH-C ₆ H ₄	150	trace	85	–
8	4-Br-C ₆ H ₄	90	73	–	16
9	2-Cl-C ₆ H ₄	90	76	–	27
10	3-NO ₂ -C ₆ H ₄	240	trace	72	–
11	4-NO ₂ -C ₆ H ₄	240	trace	61	–
12	cyclohexyl	240	90	–	27
13	1-naphthyl	50	94	–	26
14	furan-2-yl	40	96	–	24
15	CH ₃ CH ₂ CH ₂ -	240	–	–	–
16	PhCH=CH ₂	240	–	–	–

^a Isolated yield.

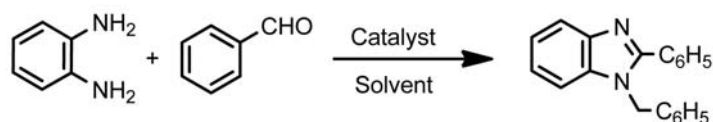
Comparison of the activity of $\gamma\text{-Fe}_2\text{O}_3@\text{SiO}_2\text{-PW}$ catalyst with those reported in the recent literature^{24–27,31} shows very good activity compared with the other catalysts (Table 3).

A suggested mechanism for the formation of 1,2-disubstituted benzimidazoles is shown in Scheme 3. The acidic sites of the catalyst react with carbonyl oxygen of aldehyde which leads to the formation of the surface-bound hydrogen-bonded species (a). Subsequent condensation of (a) with 1,2-phenylenediamine leads to the for-

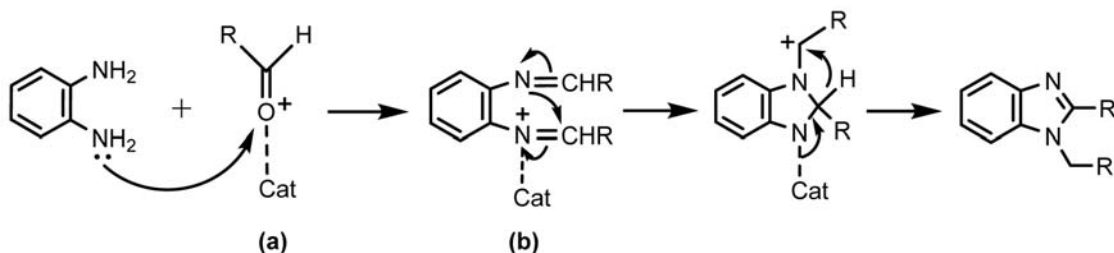
Table 1. Optimization of reaction conditions in the model reaction.

Entry	Solvent	Catalyst (mol %)	Time (min)	Yield (%) ^a	
				Product I	Product II
1	CH ₃ CN	0.07	300	12	42
2	C ₂ H ₅ OH	0.07	60	95	–
3	CHCl ₃	0.07	300	8	51
4	H ₂ O	0.07	300	–	–
5	H ₂ O/SDS (10 mg)	0.07	7	92	–
6	H ₂ O/SDS (50 mg)	0.07	5	95	–
7	H ₂ O/SDS (100 mg)	0.07	15	96	–
8	H ₂ O/SDS (10 mg)	0.03	5	21	–
9	H ₂ O/SDS (100 mg)	0.15	15	90	–
10 ^b	H ₂ O/SDS (50 mg)	0.07	60	81	12

^a Isolated yield. ^b PW was used as catalyst in this case.

Table 3. Comparison of the reaction data with other reported methods.

Entry	Catalyst	Conditions	Time	Yield (%)
1	$\gamma\text{-Fe}_2\text{O}_3\text{@SiO}_2\text{-PW}$ (0.07 mol %)	$\text{H}_2\text{O}/\text{SDS}$, r.t.	5 min	95
2	Mixed metal oxide nano crystals (5 wt% of 1,2-phenylenediamine)	CH_3CN , 60 °C	12 min	84 ²⁴
3	nano In_2O_3 (5 mol %)	CH_3CN , 60 °C	2 h	89 ²⁵
4	Iron(III)sulfate-silica (1 g)	solvent-free, r.t.	2 h	89 ²⁶
5	Resin bound hexafluorophosphate (100 mg)	water/methanol (1:1), r.t.	1 h	96 ²⁷
6	L-proline (10 mol %)	CHCl_3 , r.t.	5 h	95 ³¹

**Scheme 3.** Suggested mechanism for the preparation of 1,2-disubstituted benzimidazoles.

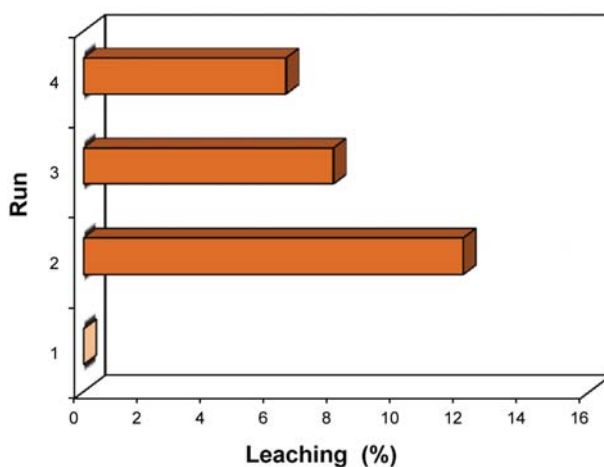
mation of imine species **(b)**. 1,3-hydride transfer and deprotonation of species **(b)** leads to the formation of 1,2-disubstituted benzimidazoles.

2. 3. Reusability of the Catalyst

Reusability of the catalyst was investigated in the model reaction (see Scheme 2). The results showed that the catalyst could be recovered and subsequently reused several times. To check the leaching of PW into the reaction mixture, the model reaction was carried out under optimized reaction conditions. After the completion of the reaction the catalyst and product were separated, and the content of PW in filtrate was evaluated quantitatively using inductively coupled plasma atomic emission spectroscopy (ICP-AES). The results showed that 26.3% of the initial PW content was leached into reaction mixture during the four successive runs (Figure 3).

Despite the leaching of PW, the yield of the product was only slightly decreased from 95% to 84% in the four subsequent catalytic cycles (Figure 4).

The acid strength and quantity of acid sites of the catalyst were examined by potentiometric titration with *n*-butylamine.¹² This method enables determination of the total number of acid sites and their distribution. As a crite-

**Figure 3.** Leaching of the catalyst during the four subsequent runs of the model reaction (reaction conditions: 1,2-phenylenediamine (1.0 mmol), benzaldehyde (2.0 mmol), catalyst (0.07 mol %), SDS (0.05 g), H_2O (5 mL), 5 min, r.t.).

riion for interpreting of the obtained results, the initial electrode potential (E_i) was taken to indicate the maximum acid strength of the sites. The number of millimoles of amine per gram of solid needed to reach the plateau in-

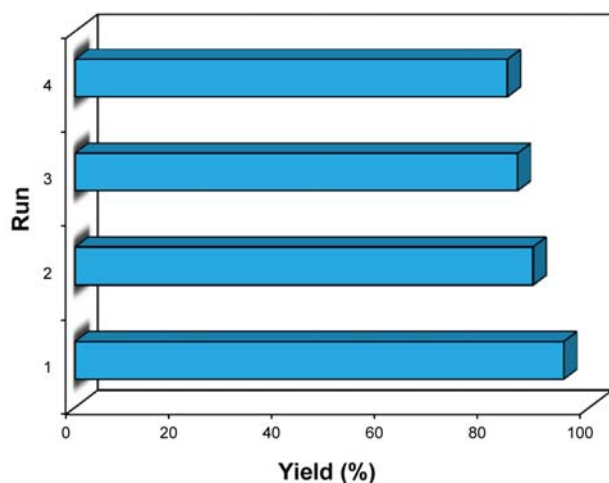


Figure 4. Change of the activity of the catalyst during the four subsequent runs of the model reaction (reaction conditions: 1,2-phenylenediamine (1.0 mmol), benzaldehyde (2.0 mmol), catalyst (0.07 mol %), SDS (0.05 g), H₂O (5 mL), 5 min, r.t.).

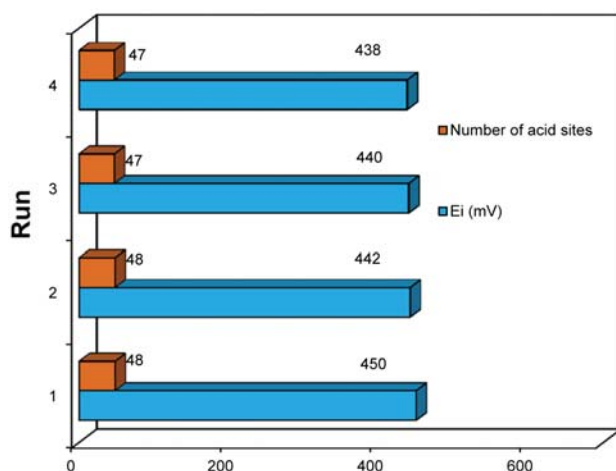


Figure 5. Change of the acidity of the catalyst during the four subsequent runs of the model reaction (reaction conditions: 1,2-phenylenediamine (1.0 mmol), benzaldehyde (2.0 mmol), catalyst (0.07 mol %), SDS (0.05 g), H₂O (5 mL), 5 min, r.t.).

indicated the total number of acid sites. The potentiometric titration results showed that most of the acid sites were preserved during four catalytic cycles (Figure 5).

3. Experimental

3.1. General

All chemicals were purchased from Fluka, Aldrich and Merck companies and were used without further purification. Transmission electron microscopy (TEM) was performed using a TEM microscope (Philips CM 120 kV, the Netherlands). X-ray diffraction (XRD) was carried out on a Bruker D8 Avance diffractometer (Germany). The

morphology of supported catalyst was observed using a scanning electron microscope (SEM) model XL30 (Philips). The tungsten (W) content was determined through inductively coupled plasma atomic emission spectroscopy (ICP-AES), using a Spectro Ciros CCD spectrometer. Surface area of the catalyst was measured using nitrogen physisorption on a Micromeritics ASAP 2000 instrument. The potential variation was measured with a Hanna 302 pH meter and a double-junction electrode. ¹H and ¹³C NMR spectra were recorded on a Bruker Avance 200 spectrometer using DMSO-*d*₆ as the solvent and tetramethylsilane (TMS) as the internal standard. Mass spectra were determined using an Agilent 6890N GC-MS instrument. Melting points were determined using a digital Galenkamp apparatus and are uncorrected.

3.2. Catalyst Preparation

The catalyst was prepared by immobilization of 40 wt.% of PW on the surface of γ -Fe₂O₃@SiO₂ NPs.¹² FeCl₂·4H₂O (2.0 g) and FeCl₃·6H₂O (5.4 g) were separately dissolved in water (20 mL). The two iron salt solutions were mixed together under vigorous stirring and diluted NH₄OH solution (0.6 M, 200 mL) was subsequently added to the stirred mixture at room temperature, followed by the addition of a concentrated NH₄OH solution (25% w/w, 30 mL) to maintain the reaction pH between 11 and 12. The resulting black dispersion was continuously stirred for 1 h at room temperature. This mixture was subsequently heated to reflux temperature for 1 h to yield a brown dispersion. The obtained γ -Fe₂O₃ NPs were purified and washed with four repeated centrifugation, decantation and re-dispersion cycles, until a stable brown magnetic dispersion with pH = 9.2 was obtained.

For preparation of γ -Fe₂O₃@SiO₂ NPs, a dispersion of the purified γ -Fe₂O₃ NPs (8.5% w/w, 20 mL) was mixed with ethanol (80 mL) and stirred for 1 h at 40 °C. A concentrated ammonia solution was added and the resulting mixture was stirred at 40 °C for another 30 min. Subsequently, TEOS (1.0 mL) was charged to the reaction vessel and the mixture was continuously stirred at 40 °C for 24 h. The γ -Fe₂O₃@SiO₂ NPs were collected using permanent magnet and washed three times with ethanol, diethyl ether and dried in a vacuum for 24 h.

For preparation of γ -Fe₂O₃@SiO₂-PW catalyst, 0.3 g of PW was dissolved in acetonitrile (50 mL). This solution was added to γ -Fe₂O₃@SiO₂ (0.25 g) and dispersed by sonication. The mixture was stirred at 60 °C for 24 h under vacuum, and obtained catalyst was collected by permanent magnet, dried in vacuum overnight and calcined at 250 °C for 2 h.

3.3. Acidity Measurement

For the potentiometric titration, 0.05 g of solid was suspended in acetonitrile (90 mL) and stirred for 3 h. The

suspension was titrated with 0.05 N solution of n-butylamine in acetonitrile. The potential variation was measured with a Hanna 302 pH meter using a double junction electrode.

3. 4. Preparation of 1,2-Disubstituted Benzimidazole

In a typical procedure, $\gamma\text{-Fe}_2\text{O}_3\text{@SiO}_2\text{-PW}$ (0.07 mol %) was added to a mixture of 1,2-phenylenediamine (1.0 mmol, 0.10 g), benzaldehyde (2.0 mmol, 0.21 g) and SDS (0.05 g) in H_2O (5 mL). The mixture was stirred at room temperature. The reaction progress was monitored by thin-layer chromatography (TLC). After completion of the reaction, the catalyst was separated from the mixture using an external magnet attached onto the reaction vessel, followed by decantation of the reaction mixture. The reaction mixture was diluted with dichloromethane and the organic layer was separated, dried over anhydrous sodium sulfate, filtered, and concentrated. The residue was purified by crystallization from ethanol to afford the pure product. All products were characterized by analytical and spectroscopic data, and compared to those reported in the literature as presented below.

1-Benzyl-2-phenyl-1H-benzo[d]imidazole (Table 2, entry 1):¹⁶ m.p. = 132–134 °C. ¹H NMR (200 MHz, $\text{DMSO-}d_6$): δ 5.21 (s, 2H), 7.11–7.55 (m, 13H), 7.71 (d, $J = 8.1$ Hz, 1H) ppm. ¹³C NMR (200 MHz, $\text{DMSO-}d_6$): δ 47.7, 110.1, 119.2, 121.8, 122.4, 125.1, 127.3, 128.1, 128.4, 128.5, 129.2, 135.3, 135.7, 142.1, 153.2 ppm. MS (m/z): 284 (M)⁺.

1-(4-Chlorobenzyl)-2-(4-chlorophenyl)-1H-benzo[d]imidazole (Table 2, entry 2):²⁵ m.p. = 135–137 °C. ¹H NMR (200 MHz, $\text{DMSO-}d_6$): δ 5.22 (s, 2H), 7.15–7.52 (m, 11H), 7.73 (d, $J = 8.1$ Hz, 1H) ppm. ¹³C NMR (200 MHz, $\text{DMSO-}d_6$): δ 48.5, 110.7, 120.1, 122.9, 123.2, 129.4, 130.1, 130.5, 130.9, 131.6, 133.7, 134.6, 135.9, 140.7, 154.8 ppm. MS (m/z): 352 (M)⁺.

1-(4-Isopropylbenzyl)-2-(4-isopropylphenyl)-1H-benzo[d]imidazole (Table 2, entry 3):²⁶ m.p. = 174–176 °C. ¹H NMR (200 MHz, $\text{DMSO-}d_6$): δ 1.24 (s, 12H), 3.16 (s, 2H), 5.20 (s, 2H), 6.98–7.40 (m, 11H), 7.70 (d, $J = 8.1$ Hz, 1H) ppm. ¹³C NMR (200 MHz, $\text{DMSO-}d_6$): δ 23.8, 24.1, 30.8, 31.5, 48.1, 110.6, 119.8, 122.4, 122.8, 126.2, 127.5, 129.7, 130.1, 132.1, 134.1, 140.5, 146.7, 148.9, 154.7 ppm. MS (m/z): 368 (M)⁺.

1-(4-methylbenzyl)-2-(p-tolyl)-1H-benzo[d]imidazole (Table 2, entry 4):¹⁶ m.p. = 128–130 °C. ¹H NMR (200 MHz, $\text{DMSO-}d_6$): δ 2.31 (s, 3H), 2.38 (s, 3H), 5.35 (s, 2H), 6.96–7.54 (m, 11H), 7.81 (d, $J = 8.0$ Hz, 1H) ppm. ¹³C NMR (200 MHz, $\text{DMSO-}d_6$): δ 21.1, 21.4, 48.4, 110.6, 120.0, 122.6, 123.4, 126.0, 127.1, 129.3, 129.7,

130.1, 133.5, 136.0, 137.5, 140.1, 154.6 ppm. MS (m/z): 312 (M)⁺.

4-(1-(4-(dimethylamino)benzyl)-1H-benzo[d]imidazol-2-yl)-N,N-dimethylaniline (Table 2, entry 5):¹⁶ m.p. = 142–144 °C. ¹H NMR (200 MHz, $\text{DMSO-}d_6$): δ 2.85 (s, 12H), 5.28 (s, 2H), 6.47–6.88 (m, 6H), 7.26–7.30 (m, 5H), 7.73 (d, $J = 8.1$ Hz, 1H) ppm. ¹³C NMR (200 MHz, $\text{DMSO-}d_6$): δ 40.1, 40.9, 42.1, 43.2, 48.7, 113.1, 113.7, 110.9, 120.3, 122.3, 122.7, 126.2, 127.3, 127.9, 130.2, 140.4, 141.4, 144.6, 154.6 ppm. MS (m/z): 370 (M)⁺.

3-(1-(3-hydroxybenzyl)-1H-benzo[d]imidazol-2-yl)phenol (Table 2, entry 6):²⁶ m.p. = 150–151 °C. ¹H NMR (200 MHz, $\text{DMSO-}d_6$): δ 5.21 (s, 2H), 6.53–6.97 (m, 6H), 7.04–7.26 (m, 5H), 7.70 (d, $J = 8.1$ Hz, 1H), 13.01 (brs, 2H, OH) ppm. ¹³C NMR (200 MHz, $\text{DMSO-}d_6$): δ 48.9, 110.6, 112.6, 114.1, 115.6, 116.3, 119.1, 119.9, 121.7, 122.1, 122.5, 129.5, 130.0, 137.6, 139.0, 140.5, 154.5, 157.1, 157.7 ppm. MS (m/z): 316 (M)⁺.

2,2'-((1,2-phenylenebis(azanilylidene))bis(methanilylidene))diphenol (Table 2, entry 7, Product II): m.p. = 158–160 °C. ¹H NMR (200 MHz, $\text{DMSO-}d_6$): δ 6.68–7.11 (m, 10H), 7.31–7.48 (m, 2H), 8.40 (s, 2H), 13.01 (brs, 2H, OH) ppm. ¹³C NMR (200 MHz, $\text{DMSO-}d_6$): δ 115.4, 115.9, 117.8, 120.4, 122.1, 127.2, 128.1, 129.7, 131.6, 144.1, 156.8, 162.9 ppm. MS (m/z): 316 (M)⁺.

1-(4-bromobenzyl)-2-(4-bromophenyl)-1H-benzo[d]imidazole (Table 2, entry 8):¹⁶ m.p. = 134–136 °C. ¹H NMR (200 MHz, $\text{DMSO-}d_6$): δ 5.21 (s, 2H), 6.95–7.49 (m, 11H), 7.70 (d, $J = 8.1$ Hz, 1H). ¹³C NMR (200 MHz, $\text{DMSO-}d_6$): δ 48.4, 110.6, 120.0, 120.4, 121.9, 122.4, 123.1, 129.3, 131.2, 131.9, 132.4, 135.3, 136.5, 140.6, 154.7. MS (m/z): 442 (M)⁺.

1-(2-chlorobenzyl)-2-(2-chlorophenyl)-1H-benzo[d]imidazole (Table 2, entry 9):²⁷ mp 161–163 °C. ¹H NMR (200 MHz, $\text{DMSO-}d_6$): δ 5.21 (s, 2H), 7.08–7.41 (m, 11H), 7.70 (d, $J = 8.1$ Hz, 1H) ppm. ¹³C NMR (200 MHz, $\text{DMSO-}d_6$): δ 41.0, 110.5, 119.8, 122.1, 122.6, 126.1, 126.7, 127.0, 128.7, 129.3, 129.8, 130.5, 132.0, 134.1, 136.5, 138.0, 140.5, 154.8 ppm. MS (m/z): 352 (M)⁺.

N,N'-(1,2-phenylene)bis(1-(3-nitrophenyl)methanimine) (Table 2, entry 10, Product II): m.p. = 167–169 °C. ¹H NMR (200 MHz, $\text{DMSO-}d_6$): δ 7.25–7.37 (m, 4H), 7.95–8.31 (m, 6H), 8.41 (s, 2H), 8.46–8.53 (m, 2H) ppm. ¹³C NMR (200 MHz, $\text{DMSO-}d_6$): δ 115.5, 122.2, 123.6, 124.4, 125.2, 128.1, 128.9, 131.8, 134.0, 144.2, 149.9, 162.7 ppm. MS (m/z): 374 (M)⁺.

N,N'-(1,2-phenylene)bis(1-(4-nitrophenyl)methanimine) (Table 2, entry 11, Product II): m.p. = 188–190 °C. ¹H NMR (200 MHz, $\text{DMSO-}d_6$): δ 7.23–7.41 (m, 4H),

7.62–7.78 (m, 4H), 8.10–8.30 (m, 4H), 8.41 (s, 2H) ppm. ^{13}C NMR (200 MHz, DMSO- d_6): δ 115.3, 122.1, 123.2, 123.9, 124.2, 128.1, 129.2, 129.7, 135.8, 144.3, 151.5, 162.8 ppm. MS (m/z): 374 (M)⁺.

2-cyclohexyl-1-(cyclohexylmethyl)-1H-benzo[d]imidazole (Table 2, entry 12):²⁷ Yellow oil. ^1H NMR (200 MHz, DMSO- d_6): δ 0.81–1.96 (m, 22 H), 3.98 (s, 2H), 7.31–7.45 (m, 3H), 7.72 (d, J = 8.1 Hz, 1H) ppm. ^{13}C NMR (200 MHz, DMSO- d_6): δ 26.1, 26.7, 27.0, 28.7, 30.1, 31.2, 33.4, 33.8, 48.2, 110.4, 119.7, 121.9, 122.5, 140.5, 154.2 ppm. MS (m/z): 296 (M)⁺.

2-(naphthalen-1-yl)-1-(naphthalen-1-ylmethyl)-1H-benzo[d]imidazole (Table 2, entry 13):²⁶ m.p. = 158–160 °C. ^1H NMR (200 MHz, DMSO- d_6): δ 5.58 (s, 2H), 6.98–7.72 (m, 18H) ppm. ^{13}C NMR (200 MHz, DMSO- d_6): δ 48.1, 110.3, 119.2, 121.9, 122.7, 123.6, 124.1, 125.3, 125.8, 126.1, 126.7, 127.1, 127.9, 128.3, 128.8, 131.8, 132.9, 133.8, 140.4, 153.7 ppm. MS (m/z): 384 (M)⁺.

2-(furan-2-yl)-1-(furan-2-ylmethyl)-1H-benzo[d]imidazole (Table 2, entry 14):²⁴ m.p. = 92–94 °C. ^1H NMR (200 MHz, DMSO- d_6): δ 5.08 (s, 2H), 5.94–6.31 (m, 4H), 7.11–7.36 (m, 5H), 7.68 (d, J = 8.1 Hz, 1H) ppm. ^{13}C NMR (200 MHz, DMSO- d_6): δ 42.1, 104.7, 105.1, 109.5, 110.5, 111.1, 119.7, 122.2, 122.7, 140.4, 140.8, 141.5, 151.7, 154.6, 155.5 ppm. MS (m/z): 264 (M)⁺.

3. 5. Reusability of $\gamma\text{-Fe}_2\text{O}_3\text{@SiO}_2\text{-PW}$ Catalyst

The reusability experiments were performed using the reaction of 1,2-phenylenediamine (20 mmol, 2.0 g) and benzaldehyde (40 mmol, 4.2 g) in the presence of 0.10 g of the catalyst in water. When the reaction was completed, $\gamma\text{-Fe}_2\text{O}_3\text{@SiO}_2\text{-PW}$ was placed on the side wall of the reaction vessel with the aid of an external magnet and separated by decantation of the reaction mixture. The remaining catalyst was washed with diethyl ether and dried in a vacuum, and reused in the next run. The acid strength and number of acid sites of the reused catalyst were measured by potentiometric titration. The content of PW in reaction mixture was evaluated quantitatively by ICP-AES.

4. Conclusions

In summary, an improved methodology for the synthesis of 1,2-disubstituted benzimidazoles has been reported using a recoverable heteropoly acid-based magnetic nano catalyst. The use of water as the solvent, low catalyst loading, mild reaction conditions, simple work-up, isolation of highly pure products in excellent yields, and

catalyst recyclability are the main advantages, which make this method practical for the synthesis of benzimidazol derivatives.

5. Acknowledgements

The authors thank the Razi University Research Council and Iran National Science Foundation (INSF) for supporting this work.

6. References

1. Y. Izumi, K. Urabe, M. Onaka, *Zeolite, Clay and Heteropoly Acid in Organic Reactions*; VCH: New York, 1993; pp. 102–150.
2. E. Rafiee, S. Eavani, F. Khajooeinejad, M. Joshaghani, *Tetrahedron* **2010**, *66*, 6858–6863.
3. E. Rafiee, M. Khodayari, S. Shahebrahimi, M. Joshaghani, *J. Mol. Catal. A: Chem.* **2011**, *351*, 204–209.
4. E. Rafiee, F. Khajooeinejad, M. Joshaghani, *Chinese Chem. Lett.* **2011**, *22*, 288–291.
5. E. Rafiee, Z. Zolfagarifar, M. Joshaghani, S. Eavani, *Synth. Commun.* **2011**, *41*, 459–467.
6. I. V. Kozhevnikov, A. Sinnema, R. J. J. Jansen, K. Pamin, H. van Bekkum, *Catal. Lett.* **1994**, *30*, 241–252.
7. J. B. Moffat, In *Metal–Oxygen Cluster Surface and Catalytic Properties of Heteropoly Oxometalates*; M. V. Twigg and M. S. Spencer, Eds.; Kluwer: New York, 2002; pp. 71–96.
8. M. Masteri-Farahani, J. Movassagh, F. Taghavi, P. Eghbali, F. Salimi, *Chem. Eng. J.* **2012**, *184*, 342–346.
9. C. S. Gill, B. A. Price, C. W. Jones, *J. Catal.* **2007**, *251*, 145–152.
10. E. Rafiee, S. Eavani, *J. Mol. Catal. A: Chem.* **2013**, *373*, 30–37.
11. Z. Zhang, F. Zhang, Q. Zhu, W. Zhao, B. Ma, Y. Ding, *J. Colloid Interface Sci.* **2011**, *360*, 189–194.
12. E. Rafiee, S. Eavani, *Green Chem.* **2011**, *13*, 2116–2122.
13. A. A. Spasov, I. N. Yozhitsa, L. I. Bugaeva, V. A. Anisimova, *Pharm. Chem. J.* **1999**, *33*, 232–243.
14. C. L. Sann, A. Baron, J. Mann, H. van den Berg, M. Gunaratnam, S. Neidle, *Org. Biomol. Chem.* **2006**, *4*, 1305–1312.
15. Y. Bansal, O. Silakari, *Bioorg. Med. Chem.* **2012**, *20*, 6208–6236.
16. P. Bandyopadhyay, M. Sathe, S. Ponmariappan, A. Sharma, P. Sharma, A. K. Srivastava, M. P. Kaushik, *Bioorg. Med. Chem. Lett.* **2011**, *21*, 7306–7309.
17. B. Yadagiri, J. W. Lown, *Synth. Commun.* **1990**, *20*, 955–963.
18. Q. Sun, B. Yan, *Bioorg. Med. Chem. Lett.* **1998**, *8*, 361–364.
19. D. M. Smith, In *Benzimidazoles and Congeneric Tricyclic Compounds*; P. N. Preston, Ed.; John Wiley & Sons, 1981; pp. 331–390.
20. A. R. Katritzky, C. W. Rees, In *Comprehensive Heterocyclic Chemistry*; M. R. Grimmett, Ed.; Pergamon: Oxford, 1984; pp. 457–498.

21. K. M. Dawood, B. F. Abdel-Wahab, *ARKIVOC* **2010**, 333–389.
22. V. R. Ruiz, A. Corma, M. J. Sabater, *Tetrahedron* **2010**, *66*, 730–735.
23. H. Yu, M. S. Zhang, L. R. Cui, *Chinese Chem. Lett.* **2012**, *23*, 573–575.
24. P. Bandyopadhyay, M. Sathe, G. K. Prasad, P. Sharma, M. P. Kaushik, *J. Mol. Catal. A: Chem.* **2011**, *341*, 77–82.
25. S. Santra, A. Majee, A. Hajra, *Tetrahedron Lett.* **2012**, *53*, 1974–1977.
26. S. Paul, B. Basu, *Tetrahedron Lett.* **2012**, *53*, 4130–4133.
27. P. Ghosh, A. Mandal, *Tetrahedron Lett.* **2012**, *53*, 6483–6488.
28. W. Stöber, A. Fink, E. Bohn, *J. Colloid Interface Sci.* **1968**, *26*, 62–69.
29. E. Rafiee, S. Eavani, S. Rashidzadeh, M. Joshaghani, *Inorg. Chim. Acta*, **2009**, *362*, 3555–3562.
31. R. Varala, A. Nasreen, R. Enugala, S. R. Adapa, *Tetrahedron Lett.* **2007**, *48*, 69–72.

Povzetek

V prispevku je opisana priprava 12-volframfosforjeve kisline kot katalizatorja na magnetnih nanodelcih, prekritih s silikagelom. Tako pripravljen katalizator so avtorji analizirali s transmisijsko elektronsko spektroskopijo, vrstično elektronsko mikroskopijo, praškovno rentgensko difrakcijo in atomsko emisijsko spektroskopijo z induktivno sklopjeno plazmo. Kislost katalizatorja so merili s potenciometrično titracijo z n-butilaminom. Katalitsko učinkovitost pripravljene katalizatorja so raziskali na modelni reakciji priprave 1,2-disubstituiranih benzimidazolnih derivatov v vodi kot topilu. Katalizator je pokazal zelo dobro katalitsko učinkovitost, saj so bili ustrezni produkti izolirani z dobrimi izkoristki pri milih reakcijskih pogojih. Katalizator je mogoče enostavno ločiti iz reakcijske zmesi z uporabo zunanjega magneta in večkrat uporabiti. Avtorji so študirali tudi puščanje katalizatorja s površine magnetnih nanodelcev in spreminjanje površinske kislosti ob večkratni uporabi.